Int. J. Electrochem. Sci., 7 **(2012)** 11338 - 11350

International Journal of
ELECTROCHEMICAL
SCIENCE
www.electrochemsci.org

Enhanced Effects of Surfactant on Sensing of Phenol on a Graphene Nano-sheet Paste Electrode

Feng-Tian Hu, Shou-Qing Liu[*]

College of Chemistry and Bioengineering; Jiangsu Key Laboratory for Environmental Functional Materials; Suzhou University of Science and Technology, Suzhou 215009, China
[*]E-mail: shouqing_liu@hotmail.com

Received: 22 August 2012 / *Accepted:* 26 September 2012 / *Published:* 1 November 2012

This article presents an enhanced sensitivity for the determination of phenol using a graphene nano-sheet paste (GNP) electrode in the presence of sodium dodecyl sulfate (SDS). The concentration of SDS, pH and other factors were examined. In pH 8.70 phosphorate buffer solution, the oxidation peak of phenol was observed at 0.67 V *vs* SCE on the GNP electrode. The relationship between peak currents and phenol concentrations is linear in the range of 8.0×10^{-8} ~ 8.0×10^{-5} mol/L, with i_p (μA) = 0.27888 + 0.04975C (μmol/L), R = 0.99926 (n = 9) and the detection limit for phenol is 5.0×10^{-8} mol/L. The electron transfer coefficiency β was evaluated to be 0.592, the standard rate constant k^0 was estimated to be 2.77×10^{-4} cm/s. The diffusion coefficiency for phenol was found to be 5.45×10^{-4} cm^2/s. This electrode has excellent reproducibility and stability in the determination of phenol in soil samples, thus, this method is expected to apply in determining the concentration of phenol in soil. A hemimicelle model was suggested to explain the enhanced current for the oxidation of phenol.

Keywords: Hemimicelle, Enhanced effect, Graphene nano-sheets, Phenol, Determination

1. INTRODUCTION

Phenols and derived phenols are known to be widespread as components in coking, pesticides, petroleum and chemical industry wastewaters. It has strong toxicity, making lands and waters polluted. Therefore, the determination of phenols in wastewaters and lands is of great significance. Some methods have been reported such as high-pressure liquid chromatography [1-3], spectrophotometry [4,5]. The electrochemical measurements also have been conducted using the modified electrodes [6-9], biosensors [10-15], quartz crystal microbalance [16] and carbon fiber electrode [17]. And the detection sensitivity and detection limit of modified electrodes and biosensors were improved by the

addition of surfactants [18-19]. These explorative efforts are of great importance for obtaining the high sensitivity and the low detection limit.

Recently, the graphene nano-sheets were extensively used as electrode materials due to its excellent electron transfer feature in electroanalytical field [20-26], and it can be functionalized via coupled with other components [27-30]. The functionalization imbues the graphene nano-sheet electrode with high sensitivity and selectivity to analytes, thus, the combination of graphene nano-sheets with specific molecules can produce unique feature, which is of great significance in analytical field.

Herein we reported on utilizing the graphene nano-sheets (GN) as electrode materials, coupled with sodium dodecyl sulfate, a surfactant, for enhancing current signals of oxidization of phenol to fabricate a sensor for the determination of phenol in soil samples polluted with phenol.

2. EXPERIMENTAL

2.1. Materials

Phenol, sodium dodecyl sulfate were purchased from Sigma-Aldrich Co. Graphite powder (average particle size = 30 μm) and paraffin oil were purchased from Shanghai Colloid Chemical Plant (Shanghai, China). All the reagents were analytical grade and used without any further purification. All solutions were prepared with 18.2 MΩ·cm deioned Milli-Q water. Diluted solutions of 0.10 mol/L phosphate buffer (PB) solution were used for pH control.

2.2. Apparatus

The cyclic voltammetric (CV) experiments were carried out with a CHI660C electrochemical workstation(CH Instrument Company, Texas, USA) in a three-electrode system at room temperature (25±2°C). A graphene nano-sheet paste (GNP) electrode was used as the working electrode, and a platinum sheet as the counter electrode, a saturated calomel electrode (SCE) as the reference electrode. All potentials are reported vs SCE. The XRD measurement was conducted with X'Pert-Pro MPD X-ray diffractometer, Panalytical, Netherland. The source of the X-ray was Cu-K (with a wavelength of 0.154 nm at a tube voltage of 40 kV, and a tube current of 40 mA. The morphological observation was performed with transmission electron microscope (TEM, TecnaiG220, FEI, USA) and scanning electronic microscopy (SEM, Quanta 400 FEG, FEI, USA). Graphene nano-sheets were dispersed in water by an ultrasonic device, and then placed on carbon-coated copper grids and dried under ambient conditions for morphological observation. Raman spectra were determined by laser size analyzer (Raman, HR 800, France).

2.3. Synthesis of graphene nano-sheets

Graphene nano-sheets were synthesized by using a modified hummers method [31]. First, the graphitic oxide was prepared by adding 1.0 g of powdered flake graphite and 0.5 g of sodium nitrate

into 23 mL of 98% sulfuric acid under stirring. The ingredients were mixed in a 250-mL beaker that had been cooled to 10 C^0 in an ice-bath. While maintaining vigorous agitation, 3.0 g of potassium permanganate was added to the suspension and the agitation was maintained for 3 h. The ice-bath was then removed and the temperature of the suspension rose to 35 C^0, where it was maintained for 35 min. At the end of 35 min, forty five milliliter of water was slowly dropped into the paste, causing violent effervescence and an increase in temperature to 98 ℃. The diluted suspension, now brown in color, was maintained at this temperature for 15 min. The suspension was then further diluted to approximately 140 mL with warm water and treated with 10% hydrogen peroxide to reduce the residual permanganate and manganese dioxide to colorless soluble manganese sulfate. Upon treatment with the hydrogen peroxide, the suspension turned bright yellow. The suspension was centrifuged, resulting in a yellow-brown paste. The paste was washed centrifugally with 5% HCl solution for three times, 95% alcohol for two times, and deioned water for three times, respectively, resulting in graphene oxide (GO) followed by dehydration at 60 C^0 *in vaco* for 12 h.

Graphene nano-sheets were obtained by reduction of GO [32]. In a typical procedure, GO (0.1 g) was loaded in a 250-mL round bottom flask and water (100 mL) was then added, yielding a uniform yellow-brown dispersion. This dispersion was sonicated using an ultrasonic bath cleaner (150 W) until it became clear with no visible particulate matter. This dispersion was warmed to 80℃, hydrazine hydrate (2.00 mL, 64.2 mmol) was then added and it was maintained in a water bath at 80℃ for 24 h. A black solid was gradually precipitated out. It was isolated by filtration over a glass funnel, washed copiously with water and methanol, and dried at 60 C^0 *in vaco* for 12 h. The product was identified as graphene nano-sheets by XRD, Roman spectra, TEM, SEM.

2.4 Preparation of GNP electrode

Mixing 60 mg of graphene nano-sheets with 180 mg of paraffin oil thoroughly in a mortar produced a uniform graphene nano-sheet paste. A portion of GNP was filled firmly into one end of a Teflon tube (d = 3 mm), and a copper wire was inserted through the opposite end to establish an electrical contact. Appropriate packing was achieved by pressing the surface against a bond paper until a smooth surface was obtained. So a GNP working electrode was obtained. Similarly, the graphite powder was used to obtain the graphite paste (GP) electrode for comparison. The resulting GNP electrode was placed in refrigerator for aging at 4 C^0 for 12 h, then it was got out and immersed in 1.0 mM $K_3Fe(CN)_6$ solution including 0.1 M KCl supporting electrolyte for estimating the effective area, the estimated area is about 0.0326 cm^2 according to Randles-Sevcik equation. The electrode was rinsed with deioned water at least for three times before used and between determinations.

3. RESULTS AND DISCUSSION

3.1 Voltammetric behaviors of phenol on GNP electrode

Curve A in Figure 1 shows the voltammetric curve of a GNP electrode in a phosphate buffer solution containing 20 μmol/L phenol and curve B shows that of a GP electrode in the same solution.

The comparison shows that the peak current generated at GNP electrode at 0.67 V is much larger than that at GP electrode in the solution, indicating the excellent electron transfer feature of the graphene nano-sheets. This electron transfer feature is attributed to the abundant edge-plane sites and defects on the graphene nano-sheets [33,34], showing the advantage of the graphene nano-sheets used as electrode materials.

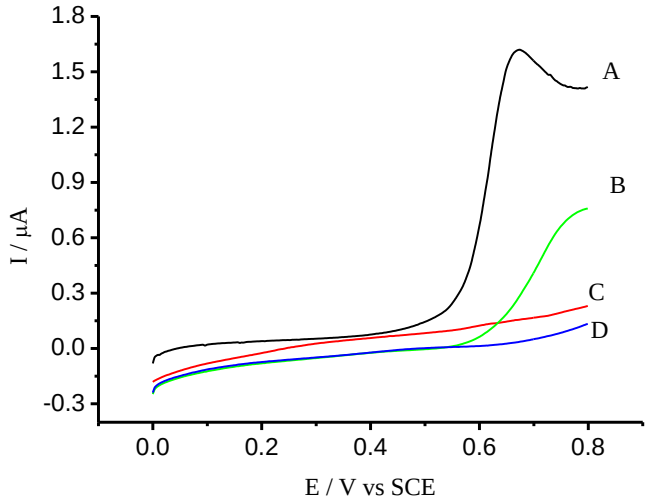

Figure 1. Linear sweep voltammetric curves of GNP and GP electrodes in 0.1 mol/L PB solution with pH 8.7 containing 20 μmol/L phenol at a rate of 100.0 mV/s. (A), GNP electrode; (B), GP electrode; (C), GNP electrode in blank PB solution without phenol; (D): GP electrode in blank PB solution without phenol.

3.2 Influence of SDS concentration on peak currents

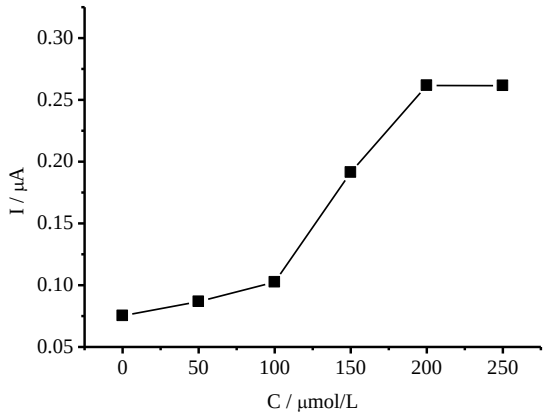

Figure 2. Influence of SDS concentration on peak currents in 0.1 mol/L PB solution containing 1.0 μmol/L phenol with pH 8.7 at a rate of 100.0mV/s.

Figure 2 shows the influence of the SDS concentrations on peak currents of phenol oxidized at GNP electrode when the concentration of phenol was maintained at a constant of 5.0 μmol/L. At the initial stage, the peak current increased as the concentration of the SDS surfactant rose. Then, the current achieved a maximum value when the SDS concentration rose to 200 μmol/L, however, the continuous addition of SDS did not lead to the current increment after 200 μmol/L. It indicates that the SDS absorption on the surface of the GNP electrode reached a saturated value at the concentration of 200 μmol/L. The enhanced effect of currents is attributed to the pre-concentration of hemicelles formed on the electrode surface to phenol in solution.

3.3 pH Choice

As known, the concentration of hydrogen ions or pH value can heavily affect the electrochemical behaviors involving in the transfer reaction of hydrogen ions. The oxidation of phenol involves forming phenoxy radicals and releasing hydrogen ions [35,36], therefore, alkali medium favors the oxidation of phenol from the viewpoint of equilibrium shift. Figure 3 shows the influence of pH values in the range of 4.0 ~ 10.0 in solution on the linear sweep voltammetric curves of phenol at the GNP electrode. As can be seen, marked oxidation peak currents were emerged in alkali medium but the peak currents disappeared in acidic medium. The maximum peak current was achieved in pH 8.7 medium whereas the current declined slightly in pH 10.0 medium. The decline may be attributed to the repulsion between the hemimicelles formed from SDS on the electrode surface and the phenoxide anions in pH > pKa medium (pKa for phenol is 9.89 [37]). SDS molecules can be adsorbed on the electrode surface to form the hemimicelles (shown in scheme 1) under potential modulation even if the SDS concentration is as low as 0.01 mmol/L [38]. When pH value of the medium is lager than pka value, phenol molecules dissociate into phenoxide anions. The negative charges on head groups of SDS repulse the anions, leading to the current decline. So the optimum pH medium is pH = 8.7, the medium was used in the following measurements.

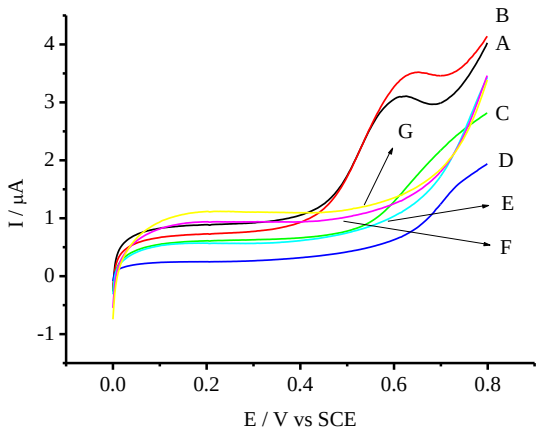

Figure 3. linear sweep voltammetric curves of GNP electrode in 0.1mol/L PB solution containing 20 μmol/L phenol and 0.2 mmol/L SDS in the potential range between 0.0V and 0.80V with different pH values at a sweep rate of 100 mV/s. (A), pH=10; (B), pH=8.7; (C), pH=8; (D), pH=7; (E), pH=6; (F), pH=5;(G), pH=4.

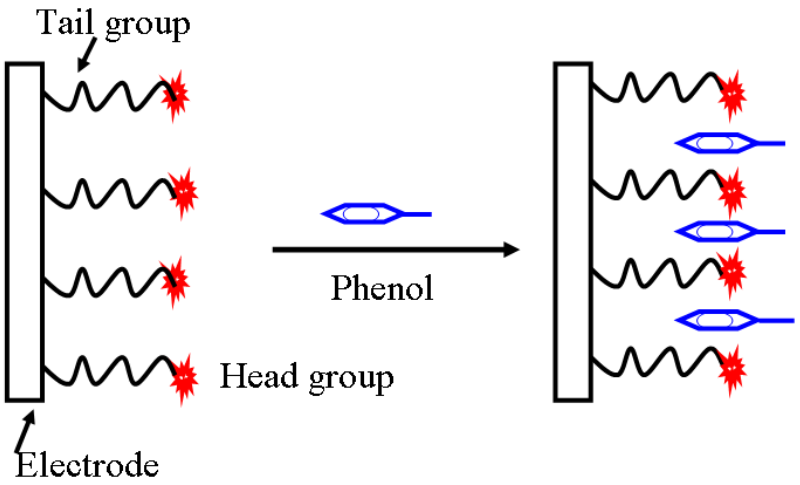

Scheme1. Hemimicelle imagine and pre-concentration for phenol.

3.4 Linearity between currents and concentrations

The as-prepared GNP electrode was exposed to various concentrations of phenol solutions for differential pulse voltammetric tests, the resulting voltammetric curves were shown in Figure 4A, accordingly, the relationship between currents and concentrations was shown in Figure 4B. As seen, the anodic peak currents increase with the analyte concentrations, and the peak currents appear a linear relationship against the phenol concentrations from 8.0×10^{-8} to 8.0×10^{-5} mol/L with R = 0.99926 (n = 9). The linear regression equation is i_p (μA) = 0.27888 + 0.04975C (μmol/L) with the detection limit of 5.0×10^{-8} mol/L. The parallel determinations for the concentration of 20.0 μmol/L phenol were performed for five times, the found mean value is 19.9 μmol/L, indicating the electrode has good reproducibility.

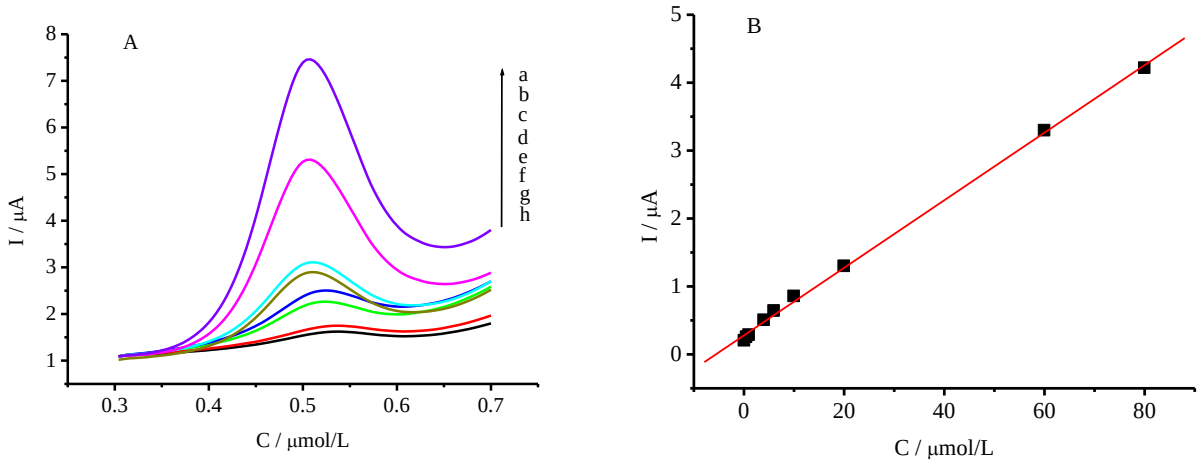

Figure 4. Differential pulse voltammetric curves of GNP electrode in 0.1 mol/L PB and 0.2 mmol/L SDS solutions containing different concentrations of phenol (a), 80 μmol/L; (b), 60 μmol/L; (c), 20 μmol/L; (d), 10 μmol/L; (e), 6 μmol/L; (f), 4 μmol/L; (g), 0.5 μmol/L; (h), 0.08 μmol/L. Potential range: 0.30 to 0.70 V; Scan rate: 100 mV/s

3.5 Interferences

To investigate the electro-catalytic selectivity of GNP electrode toward phenol, several substituted phenols were tested. They are α-naphthol, catechol, hydroquinone, 2-amino-phenol, p-chlorophenol and p-nitrophenol, respectively. The tolerable limit was defined as the concentrations of foreign substances that gave an error less than ± 5.0% in the determination of phenol. The results exhibited that, although 5 μmol/L α-naphthol, 5 μmol/L p-chlorophenol, 10 μmol/L catechol and 50 μmol/L hydroquinone have inference signals, 100 μmol/L p-nitrophenol and 100 μmol/L 2- amino-phenol have no inference signals for the determination of 5 μmol/L phenol, which means these substances can be allowed in higher concentration in the real sample. The selectivity of the method is thus acceptable and it may be applied in determining the content of phenol in soil samples.

3.6 Determination of phenol in soil samples

The recovery experiments were carried out using soil samples polluted with phenol to evaluate the accuracy of the GNP electrode for the determination of phenol. The determination for 3 real samples yielded a mean value of 4.95×10^{-6} mol/L with a mean recovery of 99.4% and a relative standard deviation of 1.57% (Table 1).

These samples were also determined with the ultraviolet-visible absorption spectrophotometry [39]. The results showed the mean concentration is equal to 4.94×10^{-6} mol/L. The concentration determined by the electrochemical method is very close to this value, confirming the GNP electrode for measuring the concentration of phenol is reliable.

Table1. Data of recovery tests

Samples	Concentration (mol/L)	Found (mol/L)	Mean value (mol/L)	Mean recovery (%)	RSD (%)
1	5.0×10^{-6}	4.87×10^{-6}	4.95×10^{-6}	99.4	1.57
2	5.0×10^{-6}	4.93×10^{-6}			
3	5.0×10^{-6}	5.06×10^{-6}			

3.7 Charge transfer coefficiency β and standard rate constant k^0

A Tafel plot (Figure 5) was drawn using background-corrected data from the rising part of the current-voltage curves (where there is not any concentration polarization) at a scan rate of 20 mV s^{-1} in order to obtain information on the number (n) of electrons involved in the rate-determining step.

$$\eta(V) = -(0.059V/n\beta)\log(i_0/A) + (0.059V/n\beta)\log|(i/A)| \quad (1)$$

On the basis of the current-voltage equation and the Tafel slope, the product of nβ is equal to 0.592.

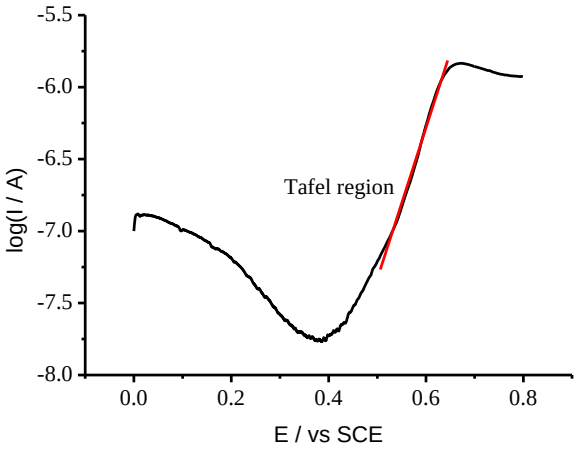

Figure 5. Tafel curve of the GNP electrode for the electrochemical oxidation of 20 μmol/L phenol in pH 8.70 PB solution .

Because the range of β is 0.3 to 0.7 [40], the value of β takes 0.296 and 0.592 when n equals 2 and 1, respectively. It is rational that n equals 1 because the number of electron transfer is estimated to be 1 according to the equation below

$$\left|E_p - E_{p/2}\right| = 2.20(RT/nF) = 56.5mV/n \qquad \text{at } 25℃ \qquad (2)$$

where the symbol E_p is the peak potential, $E_{p/2}$ the half-peak potential. The potential difference between E_p and $E_{p/2}$ was found to be 60 mV in Figure 1, leading to n = 1 in the rate-determining step of electron transfer, which is consistent with the mechanism proposed by the literature [35,36](scheme 2). The mechanism is also similar to the oxidization of vitamin B_6 [41].

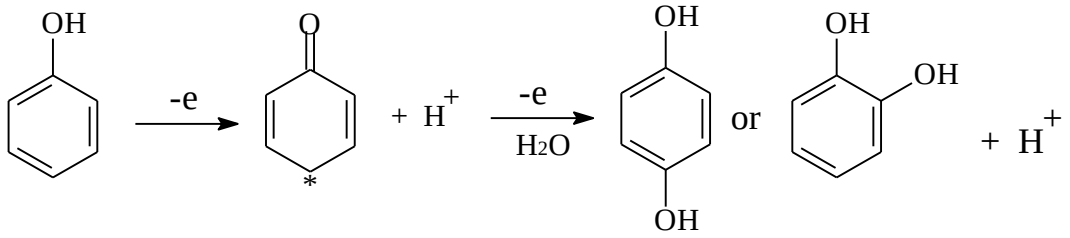

Scheme 2. Mechanism for oxidation of phenol.

Using the slope of the Tafel plot and $i_0 = nFAk^0c$ (n = 1, A = 0.0326 cm^2, F = 96500, c = 20 μmol/L and v =20 mV/s), the standard rate constant k^0 was evaluated being 2.77 × 10^{-4} cm/s.

3.11 Determination of Diffusion Coefficiency

Figure 6 shows the chronoamperometric curves of the GNP electrode in pH 8.70 PB solutions containing different concentrations of phenol. Figure 7 shows the relationship the corresponding to Figure 10 between the faradic current and the inverse of the square root of the escaped time $t^{-1/2}$. As seen in Figure 10, the current is directly proportional to $t^{-1/2}$, following Cottrell equation,

$$I = \frac{nFACD^{1/2}}{\sqrt{\pi t}} \qquad (3)$$

where D is the diffusion coefficiency (cm^2/s) and C the bulk concentration (mol/cm^3) of phenol, t the escaped time, A the effective area of the electrode (cm^2). Thus, the average value of D was found to be 5.45×10^{-4} cm^2/s.

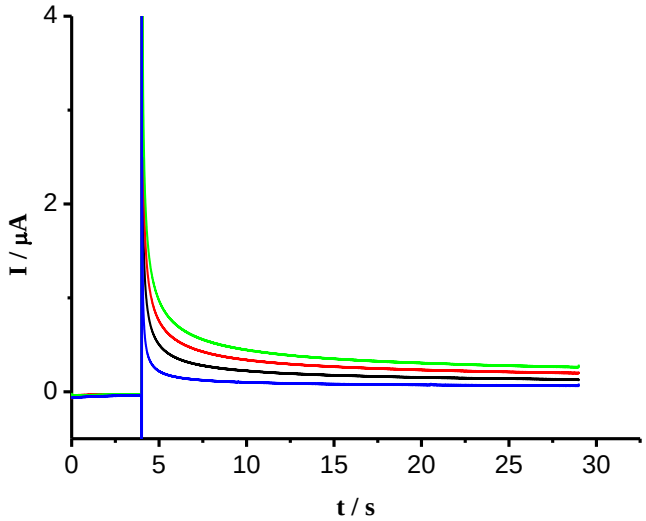

Figure 6. Chronoamperometric curves of the GNP electrode in pH 8.70 PB solutions containing (a) 0.00, (b) 6.00, (c) 12.00, (d) 18.00 μmol/L phenol, respectively. The supporting electrolyte is 0.1 mol/L KCl. The working potential was stepped from 0.00 to 0.67 V vs SCE.

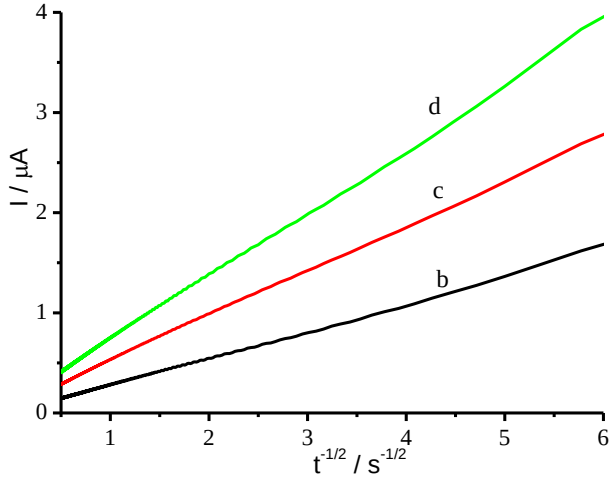

Figure 7. I – $t^{-1/2}$ curves corresponding to those in Figure 6.

4. CONCLUSION

The graphene nano-sheet paste electrode showed the advantage over the graphite paste electrode in the determination of the content of phenol. The addition of sodium dodecyl sulfate improves markedly the sensitivity to phenol. Thus, it is expected that the electrode can be applied in determining the content of phenol in soil samples in the presence of sodium dodecyl sulfate due to its reproducibility and sensitivity to phenol.

ACKNOWLEDGEMENTS
This work was financially supported by MOE Key Laboratory of Analytical Chemistry for Life Science (No. KLACLS 1013), the Opening Project of Key Laboratory of Green Catalysis of Sichuan Institutes of High Education (No. LYJ1109), the Project of Suzhou Environmental Protection Bureau (No. B201106), the Creative Project of Postgraduate of Jiangsu Province (No.CXLX11_0971), the Creative Project of Postgraduate of USTS (SKCX11S_063) and the Project Funded by the Priority Academic Program Development of Jiangsu Higher Education Institutions, China. We also thank Dr. Huang for the electroscope support of Public Center for Characterization and Test, Suzhou Institute of Nano-tech and Nano-bionics, Chinese Academy of Sciences.

References

1. R. Belloli, B. Barletta, E. Bolzacchini, S. Meinardi, *J. Chromatogr. A*, 846 (1999) 277
2. Z.K. Shihabi, R. Rauck, *J. Liq. Chromatogr.*, 14 (1991) 1691
3. B. Makuch, K. Guzda, M. Kaminski, *Anal. Chim. Acta*, 284 (1993) 53
4. W. Frenzel, S. Krekler, *Anal. Chim. Acta*, 310 (1995) 437
5. A. Uzer, E. Ercăg, R. Apak, *Anal. Chim. Acta*, 505 (2004) 83
6. I. E. Mülazımoğlu, A. D. Mülazımoğlu, E. Ylmaz, *Desalination*, 268 (2011) 227
7. Z. Mojović, N. Jović-Jovičić, A. Milutinović-Nikolić, P. Banković, A. Abu Rabi-Stanković, D. Jovanović, *J. Hazard. Mater.*, 194 (2011) 178
8. T.Spătaru, N. Spătaru, *J. Hazard. Mater.*, 180 (2010) 777
9. H. Yi, K. Wu, S. Hu, D. Cui, *Talanta*, 55 (2001) 1205
10. S. Korkut, B. Keskinler, E. Erhan, *Talanta*, 76 (2008) 1147
11. J. Adamski, P. Nowak, J. Kochana, *Electrochim. Acta*, 55 (2010) 2363
12. A. Gutés, F. Céspedes, S. Alegret, M. del Valle, *Biosens. Bioelectron.*, 20 (2005) 1668
13. H. Notsu, T. Tatsuma, A. Fujishima, *J. Electroanal. Chem.*, 523 (2002) 86
14. J. Cabaj, J. Sołoducho, A. Nowakowska-Oleksy, *Sens. Actuators B*, 143 (2010) 508
15. J. Švitel, S. Miertuš, *Environ. Sci. Technol.*, 32 (1998) 828
16. A. Mirmohseni, A. Oladegaragoze, *Sens. Actuators B*, 98 (2004) 28
17. R. M. de Carvalho, C. Mello, L. T. Kubota, *Anal. Chim. Acta*, 420 (2000) 109
18. 18.M. Hernández, L. Fernández, C. Borrás, J. Mostany, H. Carrero, *Anal. Chim. Acta*, 597 (2007) 245
19. X. G. Wang, Q. S. Wu, Y. P. Ding, *Colloids and Surfaces A*, 329 (2008) 119
20. B. Ntsendwana, B.B. Mamba, S. Sampath, O.A. Arotiba, *Int. J. Electrochem. Sci.*, 7 (2012) 3501
21. F. Li, J. Li, Y. Feng, L. Yang, Z. Du, *Sens. Actuators B*,157 (2011) 110
22. J. Ping, J. Wu, Y. Wang, Y. Ying, *Biosens. Bioelectron.*, 34 (2012) 70
23. S. Yang, D. Guo, L. Su, P. Yu, D. Li, J. Ye, L. Mao, *Electrochem. Commun.*, 11 (2009) 1912
24. M. Chao, X. Ma, Xia Li, *Int. J. Electrochem. Sci.*, 7 (2012) 2201
25. M. H. Parvin, *Electrochem. Commun.*, 13 (2011) 366
26. A. Navaee, A. Salimi, H. Teymourian, *Biosens. Bioelectron*., 31 (2012) 205
27. C. Yang, Y. Chai, R. Yuan, W. Xu, T. Zhang, F. Jia, *Talanta*, 97 (2012) 406

28. S. Yu, X. Cao, M. Yu, *Microchem. J.*, 103 (2012) 125
29. Q. Liu, X. Zhu, Z. Huo, X. He, Yo. Liang, M. Xu, *Talanta*, 97 (2012) 557
30. A. Galal, N. F. Atta, H. K. Hassan, *Int. J. Electrochem. Sci.*, 7 (2012) 768
31. S. Hummers, R. Offeman, *J. Am. Chem. Soc.*, 80 (1958) 1339
32. S. Stankovich, D. A. Dikin, R.D. Piner, K.A. Kohlhaas, A. Kleinhammes, Y. Jia, Y. Wu, S.T. Nguyen, R.S. Ruoff, *Carbon*, 45 (2007) 1558
33. I. Dumitrescu, P. R. Unwin, J. V. Macpherson, *Chem. Commun.*, (2009) 6886
34. G. P. Keeley, A. O'Neill, N. McEvoy, N. Peltekis, J. N. Coleman, G. S. Duesberg, *J. Mater. Chem.* 20 (2010) 7864
35. M.A. Maluleke, V.M. Linkov, *Sep. Purif. Technol.* 32 (2003) 377
36. T.A.Enache, A.M. Oliveira-Brett, *J. Electroanal. Chem.* 655 (2011) 9
37. F. G. Sanchez, A. N. Diaz, J.A. G. García, *Journal of Luminescence*, 65 (1995) 33
38. G. J. Besio, R. K. Prud'homme, J. B. Benziger, *Langmuir*, 4 (1988) 140
39. M. Dannis, *Sewage and Industrial Wastes*, 23 (12) (1951) 1516
40. A. J. Bard, L. R. Faulkner, Electrochemical methods, Fundamentals and Applications (2nd ed), John Wiley & Sons, INC., New York, 2001.
41. S. Liu, W. Sun, L. Li, H. Li, X. Wang, *Int. J. Electrochem. Sci.*, 7 (2012) 324

Supporting Materials

1. X-ray powder diffraction of graphene nano-sheets

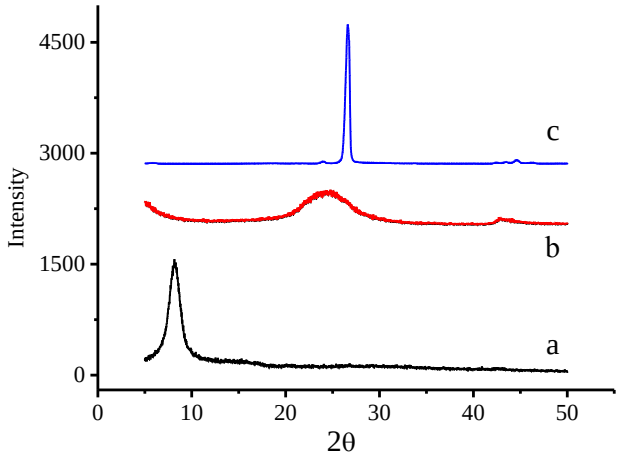

Figure 1S. XRD patterns of graphite oxide (a), graphene nano-sheets (b) and graphite (c)

2. Raman spectra of graphene nano-sheets

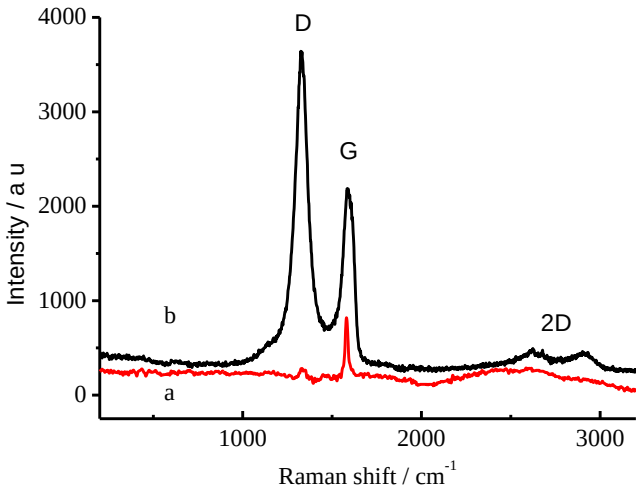

Figure 2S. Raman spectra of graphite (a) and graphene nano-sheets (b). The as-synthesized graphene nano-sheets were identified as 3 -5 layers (see the literature L. Gao, W. Ren,B. Liu, R. Saito, Z. Wu, S. Li,C. Jiang, F. Li, H. Cheng, Surface and Interference Coenhanced Raman Scattering of Graphene, ACS Nano,3(4):933-939)).

3. TEM and SEM images

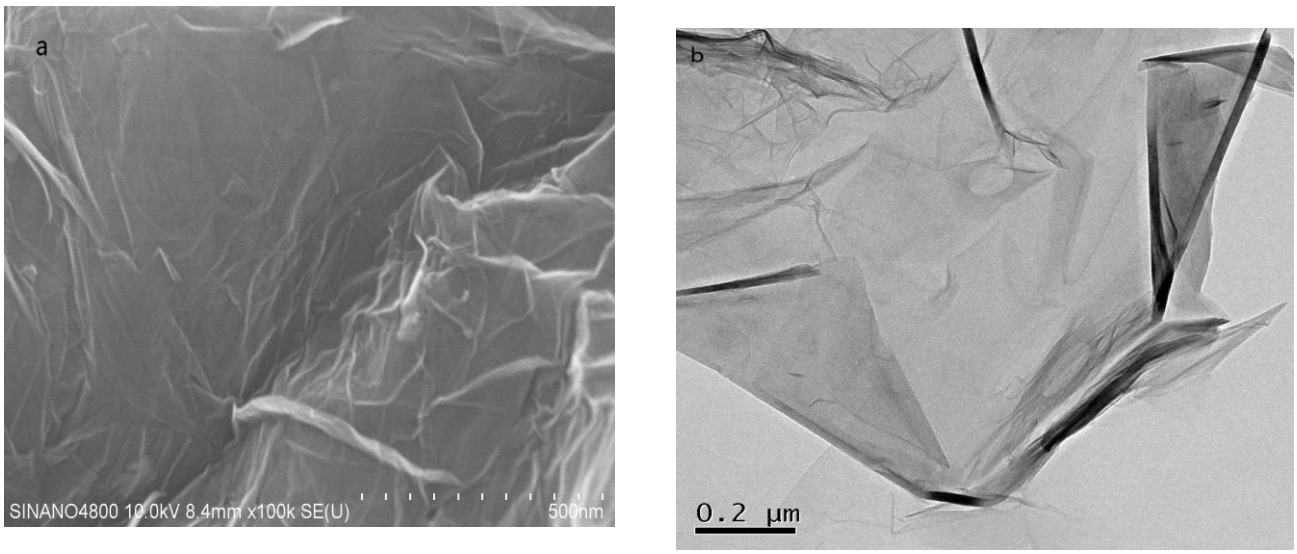

Figure 3S. The SEM (a) and TEM (b) images of graphene sheets

4. Spectroscopic quantitative measurement of phenol in soil samples polluted with phenol

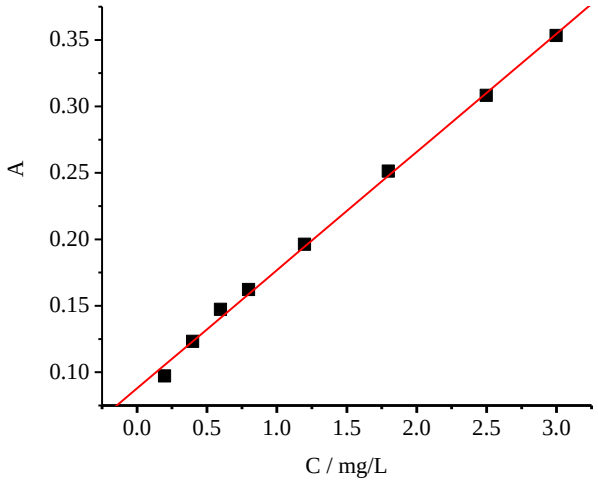

Figure 4S. The standard calibrating curve between the absorbance and the concentration of phenol. It was obtained by mixture of phenol with 4-amino antipyrine solution, and potassium ferricyanide in ammonia buffer solution. The linear equation is A= 0.08785 + 0.08897C (mg/L) with R=0.99883 (n=8) and SD=0.00477. The detailed procedures can be seen in the literature reported by Michael Dannis, *Sewage and Industrial Wastes*, 23(12) (1951)1516)

Table 1S. Data of recovery tests measured by spectrometry

Samples	Concentration(mol/L)	Found(mol/L)	Mean value (mol/L)	Mean recovery (%)	RSD(%)
1	5.0×10^{-6}	4.76×10^{-6}	4.94×10^{-6}	98.8	3.56
2	5.0×10^{-6}	4.95×10^{-6}			
3	5.0×10^{-6}	5.11×10^{-6}			